Classical Interpretation of T1rho and T2rho Relaxation

M. Carl[1], M. Bydder[2], E. Han[1], and G. Bydder[2]
[1]GE Healthcare, Waukesha, WI, United States, [2]University of California, San Diego

Introduction: $T_{1\rho}$ is a noninvasive biomarker sensitive to dipolar interactions of slow macromolecular interactions. These macromolecular motions are governed by a correlation time τ_c, which is a measure of how long the spin system takes to loose memory of the history of prior dipolar interactions. In pure liquids, the fast and random motions of the water molecules lead to very short correlation times (ns). However, since the mean dipolar fields average to zero, the overall loss of coherence is retarded, leading to the characteristically long T_2 of liquids (extreme narrowing regime). In the other limit of static magnetic field interactions (quasi-static dephasing regime), e.g. caused by magnetic susceptibility, the dephasing builds up continuously, leading to faster decay (T_2*). While these static interactions do not average away as for the fast dipolar interactions in pure water, they can be "refocused" using a spin echo pulse. Even for dephasing due to purely static susceptibility, the degree of signal recovery is reduced if an excessive amount of molecular motion (e.g. diffusion) occurs during the echo time TE. In between the two limits are tissues such as cartilage, where slow macromolecular tumbling motions have correlation times on the order of µs, which can be partially refocused by spin-locking. We present a simulation model based solely on classical equations to study spin-lattice relaxation in the rotating frame. Without the confound of a quantum mechanical treatment, this model allows for an intuitive understanding of spin-locking such as $T_{1\rho}$ dispersion, oscillations caused by residual dipolar interactions (RDI), and $T_{2\rho}$.

Theory: The spin-echo or multi-spin-echo sequence is usually described by the classical Bloch equations. $T_{1\rho}$ relaxation on the other hand is typically treated in the framework of quantum mechanics [1,2]. In a spin-lock sequence, the magnetization gets tipped into the transverse plane (usually using a 90° flip angle), followed by a constant amplitude RF pulse along the direction of the magnetization vector (see Fig1). In Fig.1a-e), several stages of the dephasing and rephasing magnetization vector as a result of the spin-lock are shown. Fig.1e shows the corresponding time evolution of the MR signal coherence, which looks similar to a conventional spin echo. The advantage to spin-locking however is that a higher spin-lock field translates into shorter refocusing times and hence more efficient refocusing of RDIs. The illustrations in Fig.4a-e show the dephasing spins remaining in a single plane. In reality, even during spin-lock the spins migrate from the plane, and the oscillation amplitude shown in Fig.4e will dampen over time ($T_{2\rho}$ decay). Once the spins are uniformly distributed around a cone, the oscillations have decayed away.

Simulations: The overall T_2* decay was modeled using Lorenzian dephasing (T_2'), and amplitude loss (T_2).

$$S(t) = \frac{1}{\pi T_2'} \exp\left(-\frac{t}{T_2}\right) \int_{-\infty}^{\infty} \frac{S(t,\omega)}{\omega^2 + (1/T_2')^2} d\omega \qquad \text{with} \qquad \frac{1}{T_2^*} = \frac{1}{T_2} + \frac{1}{T_2'} \qquad (1)$$

Two simulated $T_{1\rho}$ curves at spin-lock fields of $B_{1\rho}$ = 25 µT and $B_{1\rho}$ = 12.5 µT are shown in Fig.3a assuming $T_{1\rho} \approx$ 12ms. Several features of $T_{1\rho}$ decay are faithfully reproduced by the simulation, such as RDI oscillations and $T_{2\rho}$ decay.

Experiments: Experiments were conducted using a specialized pulse sequence shown in Fig.2 on a 1.5 inch spherical phantom with $T_2^* \approx$ 6.7ms. In order to study the magnetization behavior during the application of a spin-lock pulse, the total pulse duration TSL was incremented in 100µs steps between TR's. The mean signal intensities acquired during the data acquisition (DAQ) right after the spin-lock pulses are shown in Fig.3. In Fig.3a, the signal evolution "during" the spin-lock pulse was superimposed on the complimentary simulated data. Fig.3b shows the experimental data re-plotted by multiplying out the exponential $T_{1\rho}$ decay. Shown are the oscillations, characteristic of RDI, as well as $T_{2\rho}$ decay, which is a measure of how long the spin-locked magnetization shows distinct dephasing and rephasing patterns. Note the resemblance of the graphs in Fig.3b to a standard free induction decay, albeit at a much lower frequency of $\omega = \gamma B_{1\rho}$.

Discussion: We have shown that a simulation of relaxation mechanisms based on classical assumptions without the need for a quantum mechanical treatment is capable of reproducing many features of $T_{1\rho}$ relaxation that are usually described within the context of quantum mechanics. In particular, our simulation algorithm reproduces oscillations associated with RDI and $T_{2\rho}$ decay. Since the refocusing time for spin-locking is generally shorter than for a spin echo sequence, the relaxation time for spin-locking is generally longer than for a spin echo ($T_{1\rho} > T_2$). Fig.1 can also help explain the dispersion of $T_{1\rho}$ using different spin-lock fields strengths: The higher the field strength, the shorter the internal refocusing time, and the more the spin dephasing can be recovered before the spin system "loses memory" of prior interactions.

References: [1] Jones et al. Phys Rev **148** 1 p.332 (1966) [2] Abragam, *Principles of Nuclear Magnetism* (1961)

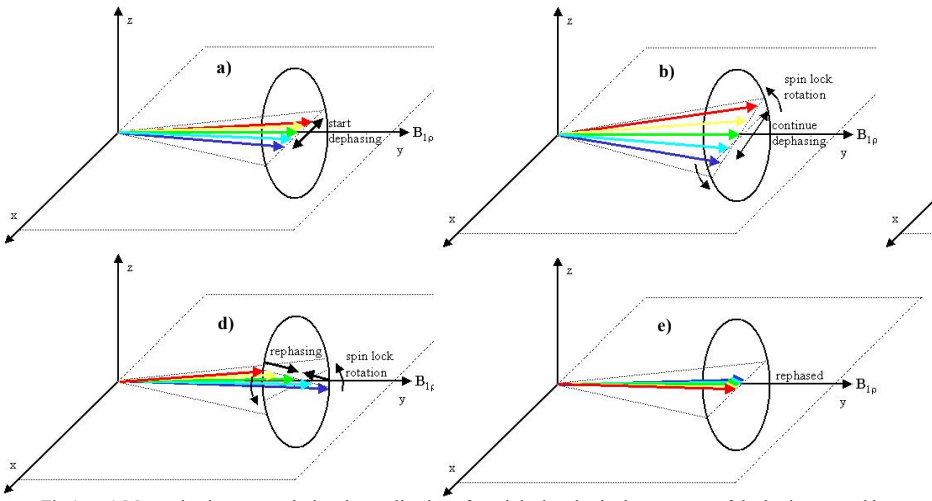

Fig.1: a-e) Magnetization vector during the application of a spinlock pulse in the presence of dephasing caused by residual dipolar interactions.f) Corresponding time evolution of transverse magnetization coherence (MR signal S).

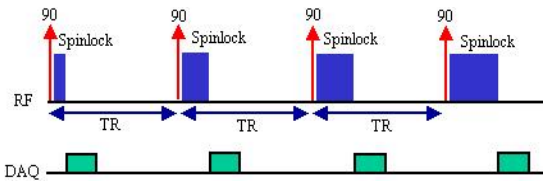

Fig.2: Pulse sequence to measure the magnetization behavior during a spinlock pulse. The duration of the spinlock pulse is incremented by 40us from TR to TR, allowing to study the magnetization behavior "during" the spinlock pulse.

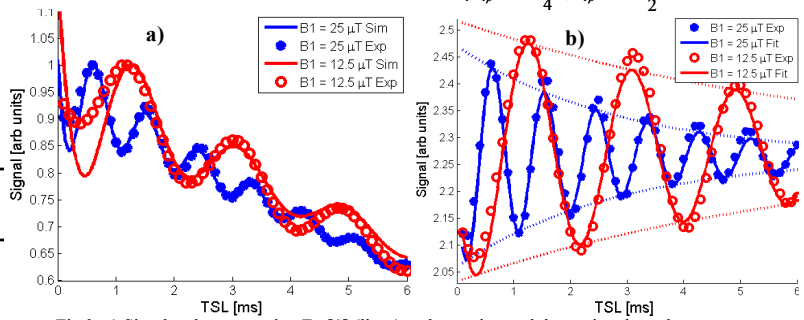

Fig.3: a) Simulated curves using Eq.[1] (lines) and experimental data using the pulse sequence in Fig.2. b) Experimental data from part a) with overall $T_{1\rho}$ decay multiplied out. Remaining are the RDI oscillation (solid lines) and $T_{2\rho}$ decay (broken lines).